

# Programming the mechanics of cohesive fiber networks by compression

## Supplementary Information

Bart E. Vos<sup>a</sup>, Luka C. Liebrand<sup>b</sup>, Mahsa Vahabi<sup>b</sup>, Andreas Biebricher<sup>b</sup>, Gijs J. L. Wuite<sup>b</sup>,  
Erwin J. G. Peterman<sup>b</sup>, Nicholas A. Kurniawan<sup>a,c</sup>, Fred C. MacKintosh<sup>b,d,e</sup>, and Gijsje H.  
Koenderink<sup>a</sup>

<sup>a</sup>Biological Soft Matter group, AMOLF, 1098XG Amsterdam, The Netherlands

<sup>b</sup> Department of Physics and Astronomy, Vrije Universiteit, 1081HV Amsterdam, The  
Netherlands

<sup>c</sup>Department of Biomedical Engineering & Institute for Complex Molecular Systems,  
Eindhoven University of Technology, 5612AZ Eindhoven, The Netherlands

<sup>d</sup>Departments of Chemical & Biomolecular Engineering, Chemistry, and Physics &  
Astronomy, Rice University, Houston, TX 77005, USA

<sup>e</sup>Center for Theoretical Biological Physics, Rice University, Houston, TX 77030, USA

### Estimation of fiber-fiber interaction strength by $\alpha$ C-regions

As explained in the main text, our findings indicate that fiber bond formation is mediated by noncovalent interactions. We hypothesize that the  $\alpha$ C-regions, two long and flexible chains which emanate from the distal ends of each fibrin monomer, are primarily responsible for this interaction, based on evidence from optical tweezers experiments showing strong interactions of these chains at the single molecule level [1]. We can estimate the total strength  $F$  of a bond between two adjacent fibers mediated by the two juxtaposed brushes of  $\alpha$ C-regions as:  $F = P * f_r * \frac{d}{l_m} * \sqrt{n_p} * 2$ . Single-molecule force spectroscopy showed that two  $\alpha$ C-regions form bonds with a binding probability  $P$  of 62% and an average rupture force  $f_r$  of 34 pN [1]). The ratio  $\frac{d}{l_m}$  is the fiber diameter  $d \approx 100$  nm divided by the length of the fibrinogen monomer,  $l_m = 45$  nm [2], and gives the number of monomers over the length of the interaction area. We multiply  $\frac{d}{l_m}$  by  $\sqrt{n_p}$ , where  $n_p$  is the total number of protofibrils in a fiber cross section (around 65 [3]), to obtain an estimate of the total number

of monomers per interaction area. Finally, the factor 2 takes into account that there are two  $\alpha$ C-regions per monomer.

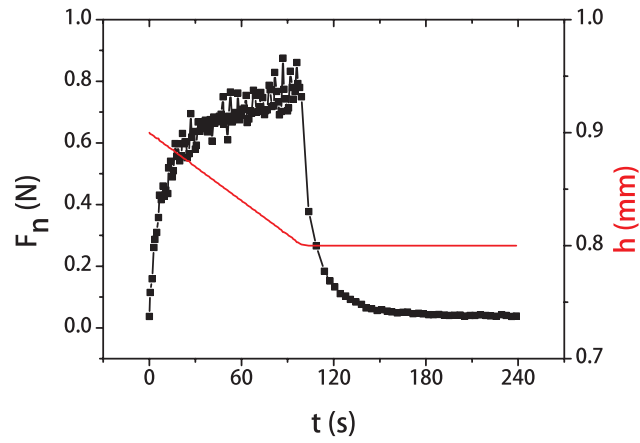
This order-of-magnitude calculation predicts a binding strength of 760 pN. Is this number large enough to make bond formation effectively irreversible even when fibrin networks are subject to a mechanical shear? To test this, we consider that for a 1% deformation of a fibrin network with shear modulus 1700 Pa (1700 Pa being the average modulus after a compression-decompression cycle for our networks) we need to apply a 17 Pa shear stress. Per characteristic area of  $2 \mu\text{m} \times 2 \mu\text{m}$  (where  $2 \mu\text{m}$  is an estimate of the pore size, or average area per fiber, based on [4]) we find that, to a first approximation, each fiber is subjected to an average force of 68 pN. Thus, we find that the newly formed connections are much stronger than the forces applied on the fibers, hence we can consider the new connections to be irreversible.

## Supplementary Movies

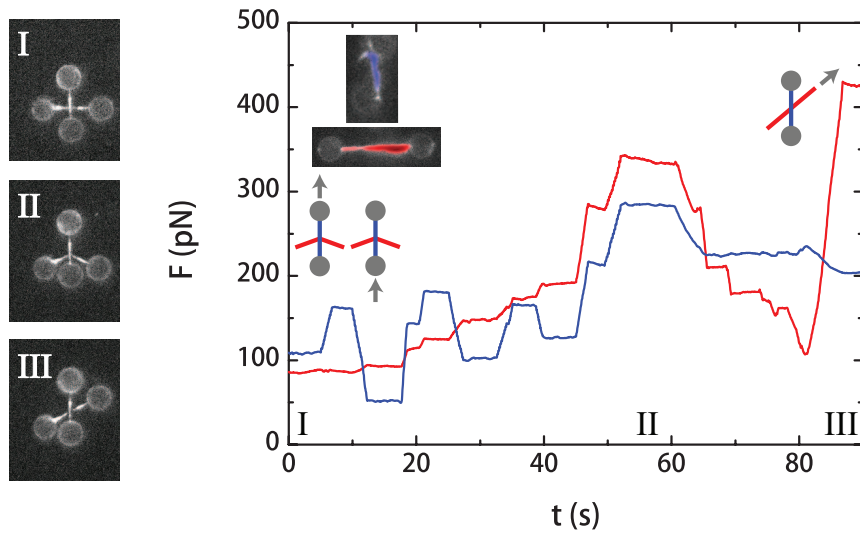
Supplementary Movie 1: **Direct measurement of the interaction between two individual fibrin fibers by optical tweezers.** A movie showing the entire time-lapse sequence of an optical tweezers experiment. After capturing two fibers, one fiber is moved vertically and placed over the other fiber. The first fiber is lowered again to bring it in contact with the horizontally oriented fiber. We confirm that a bond is formed between the two fibers by moving any of the four beads, generating fiber bending and an increase in the trapping force. The diameter of the beads is  $4.5 \mu\text{m}$ .

Supplementary Movie 2: **Two junctions merging in our computational model of cohesive fibrous networks.** A section of a simulated network during compression, starting from an initial state with no applied axial strain to the moment where the first merging event occurs.

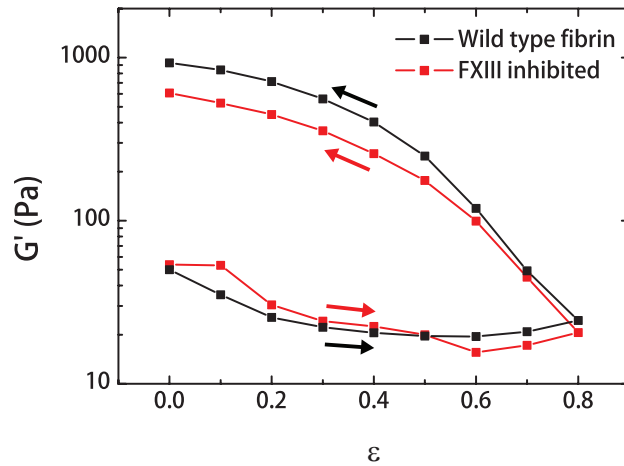
## Supplementary Figures



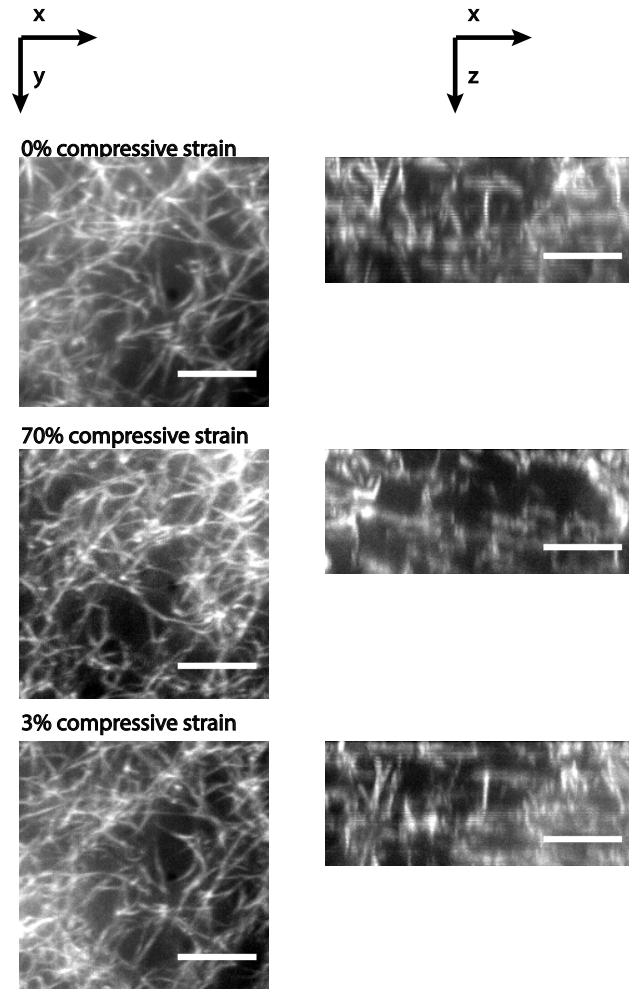
Supplementary Figure 1: The normal (axial) force  $F_n$ , exerted by the fibrin network, equilibrates over time  $t$ , after the network underwent a stepwise compression from a height  $h$  0.9 mm to 0.8 mm. A small residual normal force (see Fig. 4 in the main text) corresponds to the build-up of internal normal stresses. The corresponding sample height  $h$  is shown in red.



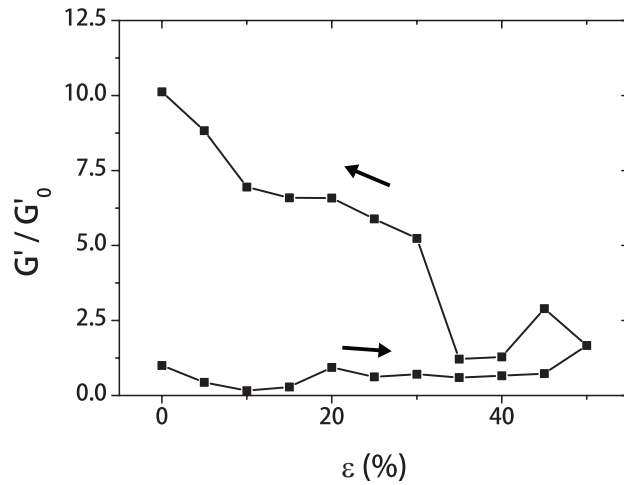
Supplementary Figure 2: Optical tweezer measurement of the interaction between two fibrin fibers in the presence of D004, a specific inhibitor for the cross-linker FXIII. The numbers above the fluorescence images (left) correspond to time points indicated in the graph (right). The colours refer to the horizontally oriented fiber (red) and the vertically oriented fiber (blue). The fibers spontaneously form a strong ( $>300$  pN) bond, indicating that bond formation does not require FXIII-mediated cross-linking.



Supplementary Figure 3: Compression and decompression of a 1 mg/ml fibrin gel, comparing cross-linked and uncross-linked networks. The black line shows the response of a control network which is cross-linked by FXIII, while the red line shows the response of a corresponding gel where FXIII-mediated cross-linking is inhibited by adding D004. The initial sample height of the FXIII-inhibited gel was 0.5 mm; in order to match the compression rate to the other experiments, where the initial height was always 1.0 mm initial, the compressive speed was adjusted to  $0.5 \mu\text{m/s}$ . Arrows indicate the sequence of the compression-decompression steps.



Supplementary Figure 4: Confocal microscopy under compression. Left column: x-y projections of a confocal recording of  $4\ \mu\text{m}$  depth; right column:  $4\ \mu\text{m}$  x-z projections of a confocal recording of  $4\ \mu\text{m}$  depth. The applied compressive strain is indicated above the respective images. In the right column, the glass cover slip is located at the top of the projection. During decompression, a small residual strain of 3% remained, due to glass bending. We observe no pronounced change in network structure after compression-decompression, indicating that only a small fraction of new bonds is created. The scale bar is  $10\ \mu\text{m}$ .



Supplementary Figure 5: Shear modulus as a function of compressive strain for a simulated network ( $\tilde{\kappa} = 10^{-3}$ ,  $d = 0.001$ ). The stiffening is lower than in Fig. 3 in the main text due to the lower value of the remodeling radius  $d$ . Another consequence of a low value of  $d$  is a relatively noisy signal since the number of new bonds is very small: an average increase in cross-linker density of 1.3% in two runs of the simulation. To this end, we averaged all data points within 5% strain intervals. Arrows indicate the sequence of the compression-decompression steps.

## References

- [1] Rustem I Litvinov, Sergiy Yakovlev, Galina Tsurupa, Oleg V Gorkun, Leonid Medved, and John W Weisel. Direct Evidence for Specific Interactions of the Fibrinogen  $\alpha$ C-Domains with the Central E Region and with Each Other. *Biochemistry*, 46(31):9133–9142, aug 2007.
- [2] W E Fowler, R R Hantgan, J Hermans, and H P Erickson. Structure of the fibrin protofibril. *Proceedings of the National Academy of Sciences of the United States of America*, 78(8):4872–4876, 1981.
- [3] Nicholas A. Kurniawan, Bart E. Vos, Andreas Biebricher, Gijs J.L. Wuite, Erwin J.G. Peterman, and Gijsje H. Koenderink. Fibrin Networks Support Recurring Mechanical Loads by Adapting their Structure across Multiple Scales. *Biophysical Journal*, 111(5):1026–1034, sep 2016.
- [4] Stefan Münster and Ben Fabry. A Simplified Implementation of the Bubble Analysis of Biopolymer Network Pores. *Biophysical Journal*, 104(12):2774–2775, 2013.